Prediction of Breakthrough Curves in Packed Beds:

C. P. JEFFRESON

Chemical Engineering Department
University of Adelaide, Adelaide, South Australia

I. Applicability of Single Parameter Models

Conditions under which simplified, single parameter models may be used to predict breakthrough curves in linear, packed bed adsorbers and thermal regenerators are examined with reference, in particular, to earlier conditions proposed by Handley and Heggs and by Babcock and co-workers. It is found that for high values of heat capacity ratio the Schumann model provides a satisfactory description of packed bed dynamics where fluids axial dispersion and solids conduction effects are lumped into a single parameter the curve spread parameter σ^*. For low values of heat capacity ratio, the equivalent conductivity model of Babcock and co-workers should provide a more accurate description. The value of the Biot number *Bi* was found to provide the sole criterion for estimating the relative importance of the internal solids conduction. Empirical correlations are presented which allow rapid estimates of breakthrough curves to be made from the curve spread parameter and which facilitate analysis of experimental data from breakthrough curve experiments.

The prediction of breakthrough curves in linear, packed-bed adsorbers and thermal regenerators has been the subject of many theoretical and experimental investigations since Schumann's work (*19*) in 1929. This interest arises fundamentally because of the economic importance of fixed bed-fluid transfer processes and because of the resultant need to rapidly and accurately design related equipment.

Design procedures for well insulated thermal regenerators or adsorbers in which particle internal conductivities may be regarded as infinite have been well developed and were summarized by McAdams (*21*). Such procedures depend on the Schumann model which makes the assumption amongst others that axial conduction or dispersion in the fluid phase is of negligible importance. The addition of a term for fluid phase axial dispersion (*5, 7*) to the Schumann equation greatly complicates the mathematical solution of the equations and raises the question of whether it is necessary to devise a completely new set of design procedures.

In this paper the conditions under which the Schumann solution may be extended to cover the cases of finite particle conductivity and axial fluids dispersion are considered. It has also been necessary to examine critically the conditions proposed earlier by Handley and Heggs (*9*) and by Babcock and co-workers (*2, 3*).

It is shown that for most cases of practical importance the well-established design procedures referred to above may continue to be used, subject to the satisfaction of a number of simple criteria. At the same time, one of the objects of this paper is to make the task of the design engineer easier by presenting empirical correlations of points on a breakthrough curve against nondimensional groups commonly used in chemical engineering. The use of these groups simplifies the tasks of design and analysis and facilitates translation of the results from heat to mass transfer.

The application of complex mathematical "models" to the determination of physical parameters of interest in the design of fixed bed processes requires an examination of the assumptions behind such models of fixed bed processes. A secondary objective of this paper is thus to suggest one method by which such models may be compared. Besides allowing evaluation of the importance of subtle effects such as boundary conditions, it should be possible to determine whether certain parameters can in fact be measured to acceptable accuracy from dynamic experiments.

ROSEN AND SCHUMANN MODELS OF PACKED BED DYNAMICS

The mathematical description or model of packed bed dynamics proposed by Rosen (*17*) has been widely applied to both thermal and mass transfer adsorbers. It is an extension of the Schumann model intended to allow for the effects of finite internal particle diffusivity. Separate equations are written for fluid and solid phases. In the present notation, the fluid phase equation becomes

$$-\frac{\partial T}{\partial z} + Y \cdot (T_s - T) = \frac{\partial T(z,t)}{\partial t} \qquad (1)$$

where $T(z,t)$ is the fluid temperature, assumed uniform across a given bed cross section at normalized distance z and normalized time t, and $T_s(z,t)$ is the average packing surface temperature which is equal in the Schumann model to the spatially uniform particle temperature. In Equation (1), distance and time have been normalized with respect to the length L of the bed and the mean fluid residence time L/v_a, respectively, where v_a is the mean interstitial fluid velocity through the bed.

The nondimensional transfer parameter Y, which links fluid and solid phases may be expressed in terms of the

Stanton number St, the bed length N in particle diameters and the mean volumetric porosity ϵ, of the packing

$$Y = 6N\ St\ (1 - \epsilon) \tag{2}$$

where $N = L/d_p$.

Spherical or right cylindrical particles have been assumed and fluid phase axial dispersion is supposed to have negligible effect.

A heat balance over the particles at distance z yields

$$Y\ (T - T_s) = V_H \frac{d\overline{T}_p(z, t)}{dt} \tag{3}$$

where $\overline{T}_p(z, t)$ is the volumetrically-averaged particle temperature which for the Schumann model is simply equal to $T_s(z, t)$. In Equation (3) the parameter V_H is the heat capacity ratio or ratio of bulk volumetric packing (thermal) capacitance to that of the fluid in the voids:

$$V_H = \frac{\rho_s \cdot c_s \cdot (1 - \epsilon)}{\rho_f \cdot c_f \cdot \epsilon} \tag{4}$$

This parameter, which may be regarded as analogous to the slope of the adsorption isotherm in mass transfer work, will be shown to be an important parameter in deciding the applicability of various models.

To complete the description in the case of the Rosen model, equations describing internal particle thermal diffusion are written, assuming uniform surface temperature. They yield with Equation (3) the relation between fluid temperature and surface temperature. The ratio

$$\frac{T_s(z, s)}{T(z, s)} = G_p(s)$$

(that is, the ratio of the Laplace transforms of surface temperature to fluid temperature for zero initial conditions) is defined as the fluid-particle transfer function and may be simply related (*14*) to the admittance functions of Rosen. Hotta (*22*) and others (*11*) have derived transfer functions for various regular packing shapes.

The fundamental parameter in these particle transfer functions is the Biot number Bi, which for heat transfer may be expressed in terms of the superficial particle Reynolds number Re_p, Prandtl number Pr, and the fluid and solid thermal conductivities k_f and k_s:

$$Bi = \frac{h_p d_p}{2\,k_f} = St \cdot Re_p \cdot Pr \left[\frac{k_f}{2\,k_s}\right]. \tag{5}$$

When the Biot number approaches zero, particle temperatures may be regarded as uniform and the Rosen model becomes identical to that of Schumann for which model many solutions are available.

Analogous nondimensional quantities may be defined for mass transfer.

EFFECTS OF INTERNAL PARTICLE CONDUCTIVITY

An alternative parameter known as the *bed length parameter*, γx has been used by Rosen and Babcock et al. (*2, 3*) as a measure of the relative importance of internal particle conduction. This parameter, also known as the "effective bed length," is simply the ratio of the transfer parameter Y to the particle Biot number

$$\gamma x = \frac{Y}{Bi} = \frac{12N(1 - \epsilon) \cdot k_s}{Re_p \cdot Pr \cdot k_f} \tag{6}$$

Handley and Heggs (*9*) have suggested that internal particle conduction effects may be ignored when the value of the bed length parameter is greater than 60. In this case according to their numerical computations, the Schumann solution becomes applicable to high accuracy. On the other hand, Bradshaw et al. (*4*) have suggested that solids diffusion be allowed for by defining, in Handley and Heggs' terminology (*8*), a pseudo Stanton number and hence heat transfer parameter Y_p which could be used in the Schumann model

$$\frac{1}{Y_p} = \frac{1 + Bi/5}{Y} \tag{7}$$

This suggestion may be shown to be more nearly correct. Thus, equations have been derived by various workers for the first three cumulants, κ_n of the chromatographic or impulse response $g(t)$ of a packed bed for the more general case which includes axial fluid phase dispersion (*11, 15, 18, 20*). The first cumulant κ_1 is the first absolute moment μ'_1 or stoichiometric time for a breakthrough curve. It is independent of transfer parameters on the time scale of Equations (1) and (3)

$$\mu_1' = 1 + V_H$$

or in real time units:

$$\mu(t) = \mu_1' \cdot \frac{L}{v_a} = (1 + V_H)\frac{L}{v_a}$$

$$= \frac{M_s c_s + M_f c_f}{W \cdot c_f}$$

where $\mu(t)$ is the stoichiometric time in minutes, M_s is the total mass of packing, M_f is the total mass of interstitial fluid and W is the weight flow rate of fluid in (say) pounds per minute.

(The reader is reminded that the breakthrough curve is defined by a plot of the integral of the impulse response against time.) The dispersion or *spread* of either curve about the stoichiometric time may be defined intuitively in terms of the standard deviation σ of the impulse response. The square of this, the variance, second central moment, or second cumulant κ_2 becomes for negligible axial fluids dispersion

$$\kappa_2 = \sigma^2 = \frac{2}{Y}(\mu_1' - 1)^2 \cdot (1 + Bi/5) = \frac{2V_H^2}{Y_p}$$

from (7),

or, normalizing time with respect to the first moment:

$$\kappa_2^* = \sigma^{*2} = \frac{2\beta^2}{Y} \cdot (1 + Bi/5) \tag{8}$$

where β is the ratio of the solid packing thermal capacitance to that of the packing plus fluid.

$$\beta = \frac{V_H}{V_H + 1} = \frac{\rho_s c_s (1 - \epsilon)}{\rho_s c_s (1 - \epsilon) + \rho_f c_f \epsilon} \tag{9}$$

According to Equation (8), the fractional increase in curve spread as measured by σ^* depends only on the value of the Biot number, so that the "effective bed length" γx is only a secondary parameter. In other words, the ratio of the curve spreads σ^* for two experiments having the same value of transfer parameter Y but differing Biot numbers, Bi_1 and Bi_2 is given (approximately) by $\sqrt{(1 + Bi_2/5)}/\sqrt{(1 + Bi_1/5)}$.

The fact that for the examples chosen by Handley and Heggs, the criterion $\gamma x > 60$ resulted in good agreement

between the Schumann and Rosen models may now be seen to be largely fortuitous, that is, the values of the Y chosen were such as to make the Biot number small when $\gamma x > 60$.

For example, consider a packed bed of "Perspex" or methyl methacrylate spheres through which air ($Pr = 0.74$) is flowing with a superficial particle Reynolds number Re_p of 1,000. Then according to the Denton correlation (6), a Stanton number of about 0.09 would be predicted. The ratio k_s/k_f of Perspex to air thermal conductivities is about 8.08 so that a particle Biot number may be estimated

$$Bi = St \cdot Re_p \cdot Pr \left[\frac{k_f}{2k_s} \right] = 4.1$$

Hence the spread σ^* of breakthrough curves about the center of mass will, according to the above analysis, be greater than that of a highly conductive material in the ratio $\sqrt{(1 + 4.1/5)} = 1.35$, or Perspex breakthrough curves will be 35% more spread out than (say) lead or copper breakthrough curves under the same flow conditions. For the above example, γx would for a porosity of 40% be given by Equation (6)

$$\gamma x = 7.86 \times 10^{-2} \times N$$

In order to satisfy Handley and Heggs' criterion we would require the bed length N to be about 760 diameters. In this case, the Handley and Heggs' criterion would predict particle conduction effects to be absent, while the present theory shows that breakthrough curves would still be 35% more spread out.

The experimental evidence available for the applicability of Equation (7) to packed bed studies will be considered in the companion paper to this paper (23).

THE EQUIVALENT CONDUCTIVITY MODEL

The single parameter model derived by Babcock and coworkers (2, 3) treats the two phase medium as a single phase one, described by an effective axial Peclet number Pe_a, where for the temperature $T(z, t)$ of the fluid and solid phases

$$(1 + V_H) \frac{\partial T}{\partial t} = \frac{\partial T}{\partial z} + \frac{1}{Pe_a} \cdot \frac{\partial^2 T}{\partial z^2} \qquad (10)$$

The value of $1/Pe_a$ is computed from the sum of dispersive contributions due to (static) axial fluid-solid-fluid conduction, fluid phase axial dispersion, fluid-solid heat transfer resistance, and internal particle thermal resistivity.

Assuming for the present that the first two contributors to breakthrough curve dispersion are negligible, the Babcock formula for Pe_a becomes

$$\frac{1}{Pe_a} = \frac{1 + Bi/5}{Y} \cdot \beta^2 \qquad (11)$$

The similarity between Equations (8) and (11) arises because for simplified boundary conditions (5)

$$\kappa_2^* = \sigma^{*2} = 2/Pe_a$$

so that the variances of the equivalent conductivity and Rosen models are identical. The use of the single parameter Pe_a to describe the complex processes which occur in a packed bed is thus similar to the use of σ^* or Y_p as a parameter in the Schumann model. Since the predictions of these two simplified models may be shown to differ despite identical curve spreads the source of the difference will now be examined.

Table 1. Ratio of Skewness Coefficients γ_1 Predicted By Rosen Model to that Predicted by Schumann Model with Pseudo Heat Transfer Factor Y_p

Biot number	0	.5	1	2	4	8	16
Ratio	1.000	1.003	1.012	1.035	1.085	1.160	1.249

Table 2. Typical Heat Capacity Ratios V_H at 70°F. Bed porosity assumed: 0.40

Fluid	Pressure, lb./sq.in.gauge	Heat capacity ratio, V_H for packings indicated below: Soda glass	Perspex	Lead	Steel
Water	—	0.76	0.62	0.54	1.28
Air	0	6100	5000	4300	10300
	50	1410	1150	1000	2400
	100	800	650	560	1340
	200	420	350	300	720

BREAKTHROUGH CURVE SHAPE CRITERION

A useful criterion of impulse response or breakthrough curve *shape* as distinct from curve *spread* is the third central moment π^3 equal to third cumulant κ_3. Normalizing time as before relative to the first moment we have, for the Rosen model (14)

$$\kappa_3^* = \pi^{*3} = \frac{6\beta^3}{Y^2} \cdot \frac{2Bi^2 + 14Bi + 35}{35} \qquad (12)$$

while the corresponding equation for the Schumann model is obtained by setting $Bi = 0$ in Equation (12). If we substitute the pseudo transfer parameter for Y in the Schumann equation we obtain

$$\left.\begin{aligned} \kappa_3^* &= (6/Y^2) \cdot \beta^3 \cdot (1 + Bi/5)^2 \\ &= \frac{6\beta^3}{Y^2} \cdot \frac{Bi^2 + 10Bi + 25}{25} \\ &= \frac{6\beta^3}{Y^2} \cdot \frac{1.4Bi^2 + 14Bi + 35}{35} \end{aligned}\right\} \qquad (13)$$

which differs from Equation (12) in one term only.

The ratio of the value of κ_3^* predicted by Equation (12) to that predicted by Equation (13) is equal to the ratio of the predicted statistical *"coefficients of skewness"* and is again dependent only on the Biot number. A few values are tabulated in Table 1.

The coefficient of skewness is a measure of the asymmetry of a probability density function equivalent in this case to the impulse response $g(t)$ of a packed bed.

The same criterion may now be applied to the equivalent conductivity model. In (12) all the cumulants of this model were derived. For the third cumulant we have normalizing the time scale as before and using Equation (11)

$$\kappa_3^* = \frac{12}{Pe_a^2} = \frac{12\beta^4}{Y^2} \cdot (1 + Bi/5)^2 \qquad (14)$$

Comparing with Equations (13) for the Schumann model we see that the source of the difference lies in the second packing capacity ratio β or from (9) in the capacity ratio V_H.

When the capacity ratios V_H are allowed to become very large ($V_H \to \infty$, $\beta \to 1$) agreement between coefficients of skewness will be poor even although curve spreads

or variances are identical. When V_H is set equal to unity ($\beta = 1/2$) skewnesses will be identical.

In the experiments of Babcock and co-workers the fluids used were aqueous whereas other heat transfer workers (*4, 6, 8, 16, 19*) used gases, usually air. Heat capacity ratios differ widely between the two types of experiments as shown in Table 2.

The excellent agreement obtained by Babcock and co-workers between theory and experiment may thus be seen to be due to the low values of V_H occurring in their experiments. Similarly good agreement was obtained in the experiments of Handley and Heggs and in experimental work by the writer (*14*), using air.

Since $\beta \simeq 1$ even for pressures of 200 lb./sq.in.gauge, it is not surprising that no heat capacity ratio effect has yet been observed in heat transfer experiments using air.

The use of aqueous fluids accentuates the effects of axial fluids dispersion and a study of this effect seems to have been of primary interest in Babcock's experiments. It does seem however that the equivalent conductivity model is unlikely to be of great practical value as an approximate, simplified model of packed bed dynamics where the packing has a large adsorptive capacity.

It should be pointed out nonetheless that irrespective of the ratios of the skewnesses, the absolute value of the coefficient of skewness:

$$\gamma_1 = \kappa_3^*/\kappa_2^{*3/2} = \pi^{*3}/\sigma^{*3}$$

becomes very small for all models as $Bi \to 0$ and, more importantly as Y becomes large. For fixed flowrate γ_1 varies inversely as the square root of the bed length. Hence for γ_1 small it does not very much matter which of the three models we choose since they will all tend to become Gaussian and perfectly symmetrical.

PREDICTED EFFECTS OF AXIAL FLUIDS DISPERSION

The addition of the term $+ 1/Pe' \cdot \partial^2 T/\partial z^2$ to the left-hand side of Equation (1) is intended to allow for the effects of axial dispersion in the fluid phase where Pe' is the bed-length normalized Peclet number

$$Pe' = \frac{v_a L}{D_e} = N \cdot \frac{v_a \cdot d_p}{D_e} = N \cdot Pe.$$

D_e is a dispersion coefficient which accounts for the experimentally observable fact that when an impulsive or chromatographic change in concentration is applied to the fluid flowing through a bed of nonadsorptive or inert packing, axial spreading of the pulse occurs (*5, 7*). In heat transfer work, the phenomenum cannot be observed independently of fluid-solid transfer processes. Hence, its precise nature cannot be determined.

The Rosen model extended for axial dispersion will henceforth be called the two phase continuous model to distinguish it from both the single phase, equivalent conductivity and the two phase finite stage models.

Allowing for axial fluids dispersion, Equation (8) becomes (*5, 12*)

$$\kappa_2^* = \sigma^{*2} = \frac{2}{N\,Pe} + \frac{2\beta^2}{Y} \cdot (1 + Bi/5) \qquad (15)$$

An identical result has been obtained from the finite stage model (*11*) of packed bed dynamics when $Pe = 2$ and also by Babcock and co-workers from the equivalent conductivity model because

$$\frac{1}{Pe_a} = \frac{1}{NPe} + \frac{\beta^2}{Y} \cdot (1 + Bi/5) \qquad (16)$$

It would be useful to lump the effects of axial dispersion into an apparent heat transfer parameter Y_{calc} so that the Schumann solution could also be used for the axial dispersion case. Curve spreads for all models may be made identical if Y_{calc} is defined suitably for Schumann model so that Equation (17) and Equation (15) are made identical

$$\kappa_2^* = \sigma^{*2} = \frac{2\beta^2}{Y_{calc}} \cdot (1 + Bi_{calc}/5) \qquad (17)$$

where

$$Bi_{calc}/Y_{calc} = Bi/Y$$

and

$$\frac{\beta^2}{Y_{calc}} = \frac{1}{NPe} + \frac{\beta^2}{Y} \qquad (18)$$

Since curve spreads are now identical for all models we will again compare curve shapes. For simplicity in the equations, set Biot numbers all equal to zero. For the Schumann model, substitution of Y_{calc} from Equation (18) instead of Y in Equation (13) yields for $Bi = 0$:

$$\kappa_3^* = \pi^{*3} = 6\left[\frac{1}{N^2 \cdot Pe^2 \cdot \beta} + \frac{2\beta}{NPe \cdot Y} + \frac{\beta^3}{Y^2}\right] \qquad (19)$$

For the two phase continuous model (*12*) with $Bi = 0$:

$$\kappa_3^* = \pi^{*3} = 6\left[\frac{2}{N^2Pe^2} + \frac{2\beta^2}{NPe \cdot Y} + \frac{\beta^3}{Y^2}\right] \qquad (20)$$

which for large capacity ratio ($V_H \to \infty$, $\beta \to 1$) agrees with (19) except for the first term. Hence, good agreement may be expected, except for low Reynolds numbers ($Re_p < 10$) when Pe becomes small (*8*) and Stanton number large [since the Nusselt number should approach a constant value (*16*)].

Agreement is better in the case of the finite stage model. The normalized third cumulant then becomes (*12*)

$$\kappa_3^* = \pi^{*3} = 6\left[\frac{1.33}{N^2Pe^2} + \frac{2\beta^2}{NPeY} + \frac{\beta^3}{Y^2}\right] \qquad (21)$$

Which for large capacity ratio ($\beta \to 1$) differs only slightly from (19). In obtaining Equation (21) the effective number of mixing stages, M has been set equal to $NPe/2$ corresponding to conditions of relatively high Reynolds number (*7*) at least in the absence of interphase transfer.

MORE DETAILED MODEL COMPARISONS

A more detailed comparison of the breakthrough curve predictions of various models may be obtained by comparing the curves themselves, point by point. Such comparisons may be misleading since computational errors may exceed the differences between models.

An alternative criterion to point by point comparisons is to use the integral deviation square (or alternatively "root mean square") or difference between models. The use of Rayleigh's theorem as pointed out by Hays, Clements, and Harris (*10*) allows the root mean square deviation between models to be computed from the differences between the frequency response transfer functions of the models without obtaining actual time responses first.

A useful feature of model comparisons by this method is that complex models, the moments of which are difficult to derive, may be compared provided the frequency response transfer functions are available. The effects of subtle differences introduced by boundary conditions may also be evaluated.

In the model comparisons discussed below, the objective was to determine the range of parameters for which either the Schumann model or the equivalent conductivity model is predicted to yield a good representation of the presumably more complete "two phase continuous" or "two phase finite stage" models. An outline of the mathematical basis of the method and the transfer functions used are summarized in the present notation in Appendix 1.* In the comparisons reported, the time scale has been normalized relative to the first moment of the impulse response and the chromatographic or impulse responses have been compared instead of the breakthrough curves since these are more sensitive.

RESULTS OF INTEGRAL DEVIATION SQUARE COMPARISONS

Computations were carried out for four values of the normalized variance σ^{*2}, 0.05, 0.125, 0.25 and 0.50 corresponding to breakthrough curves ranging from sharp to diffuse. As a guide to the physical conditions which may correspond to this range of values, predicted normalized variances are given in Table 3 for heat transfer work assuming a Stanton number-Reynolds number correlation of

$$St = 0.72/Re_p^{0.30}$$

corresponding to the Denton correlation (6) extrapolated back below its valid lower limit of $Re_p = 500$. The axial dispersion Peclet number assumed was 2, with a bed porosity of 0.40. In the tabulation, highly conductive particles have been assumed. For less highly conductive particles an additional term

* Appendix 1 has been deposited as Document No. 01719 with the National Auxiliary Publications Service (NAPS), c/o CCM Information Corp., 866 Third Ave., New York 10022 and may be obtained for $4.00 for microfiche or $11.60 for photocopies.

Table 3. Approximate Values of Normalized Variance σ^{*2} for Heat Transfer in Packed Beds, $V_H = 10^4$, $\epsilon = 0.40$, $Bi = 0$

Re_p	Approx. St	$N\sigma^{*2}$	Variance σ^{*2} at Bed Lengths Indicated $N =$ 25	$N =$ 50	$N =$ 100	$N =$ 250
100	0.181	4.072	0.163	0.081	0.041	0.016
200	0.147	3.782	0.151	0.076	0.038	0.015
400	0.119	4.656	0.186	0.093	0.047	0.019
1000	0.091	6.128	0.245	0.122	0.061	0.024
2000	0.074	7.545	0.302	0.151	0.075	0.030
4000	0.060	9.290	0.372	0.186	0.093	0.037
10000	0.045	12.229	0.489	0.244	0.122	0.049

Table 4. Typical Results of Some Model Comparisons via Integral Deviation Square Computations

$\int_0^\infty [\epsilon(t^*)]^2\,dt^* = \frac{2}{\pi}\int_0^\infty R_\epsilon^2\,(\omega^*)d\omega^*$ where $\epsilon(t^*)$ is deviation between model predicted impulse responses, normalized relative to first moment and $R_\epsilon(\omega^*)$ is real part of Fourier transform of difference.

σ^{*2}	Model Parameters: (Peclet Number, $Pe = 2$) Pe_a	N	Bi	Υ	Integral Deviation Squares: Schumann A		B		Equivalent conductivity C		D	
	1. Heat capacity ratio, $V_H = 10^4$											
0.5	4.0	40	0.0	4.21	8.601	E-07	1.53	E-07	1.16	E-01	1.16	E-01
			0.2	4.38	1.18	E-06	2.99	E-07	1.16	E-01	1.16	E-01
			0.8	4.88	1.13	E-05	8.13	E-06	1.14	E-01	1.15	E-01
			2.0	5.89	1.65	E-04	1.52	E-04	1.09	E-01	1.09	E-01
0.25	8.0	20	0.0	10.00	6.01	E-04	7.56	E-05	3.72	E-01	3.91	E-01
			0.4	10.80	6.54	E-04	9.56	E-05	3.71	E-01	3.90	E-01
			1.6	13.20	1.33	E-03	4.44	E-04	3.59	E-01	3.78	E-01
			3.2	16.40	3.22	E-03	1.72	E-03	3.39	E-01	3.57	E-01
0.125	16	80	0.0	17.80	2.29	E-06	2.96	E-07	2.38	E-01	2.41	E-01
			1.0	21.33	8.87	E-06	4.08	E-06	2.34	E-01	2.37	E-01
			2.0	24.88	3.51	E-05	2.47	E-05	2.25	E-01	2.28	E-01
			4.0	31.99	1.53	E-05	1.29	E-04	2.07	E-01	2.10	E-01
0.050	40.0	80	0.0	53.3	4.90	E-06	4.27	E-06	9.52	E-03	1.04	E-02
			2.0	74.6	1.82	E-05	7.35	E-06	9.13	E-03	9.97	E-03
			4.0	96.0	5.20	E-05	1.32	E-05	8.59	E-03	9.40	E-03
			8.0	139.0	1.40	E-04	2.60	E-05	7.77	E-03	8.55	E-03
			16.0	224.0	2.89	E-04	4.54	E-05	6.90	E-03	7.63	E-03
	2. Heat capacity ratio, $V_H = 1$											
0.25	8.0	20	0.0	2.5	8.43	E-01	8.32	E-01	6.67	E-03	6.39	E-03
			0.2	2.6	8.43	E-01	8.32	E-01	6.66	E-03	6.37	E-03
			0.4	2.7	8.44	E-01	8.33	E-01	6.61	E-03	6.31	E-03
			0.8	2.9	8.46	E-01	8.35	E-01	6.45	E-03	6.12	E-03
			1.6	3.3	8.52	E-01	8.41	E-01	5.91	E-03	5.51	E-03
0.125	16.0	40	0.0	5.0	4.59	E-01	4.56	E-01	2.60	E-03	2.88	E-03
			1.0	6.0	4.61	E-01	4.58	E-01	2.40	E-03	2.64	E-03
			2.0	7.0	4.65	E-01	4.62	E-01	2.03	E-03	2.22	E-03
			4.0	9.0	4.74	E-01	4.71	E-01	1.45	E-03	1.50	E-03
0.050	40	80	0.0	13.3	5.32	E-01	5.30	E-01	1.57	E-03	1.91	E-03
			2.0	18.6	5.34	E-01	5.32	E-01	1.27	E-03	1.57	E-03
			4.0	24.0	5.38	E-01	5.36	E-01	8.94	E-04	1.14	E-03
			8.0	34.6	5.43	E-01	5.41	E-01	4.52	E-04	6.07	E-04
			16.0	56.0	5.50	E-01	5.48	E-01	1.76	E-04	2.34	E-04

$$\frac{2\beta^2}{Y} \cdot \frac{Bi}{5} = \frac{2\beta^2}{5\gamma x}$$

may be added, where γx is computed from Equation (6).

Table 4 shows a number of computed integral deviation squares between: A. Schumann model and two-phase continuous; B. Schumann model and two-phase finite stage; C. equivalent conductivity and two-phase continuous; and D. equivalent conductivity and two-phase finite stage models for capacity ratios V_H of 10^4 and 1 and several arbitrarily chosen bed lengths and a constant Peclet number of 2. The comparison is not exhaustive but does illustrate the advantage of the method.

As may be seen from Table 4, the Schumann approximation is clearly superior to the equivalent conductivity model for the high value of V_H while the situation is reversed for the low capacity ratio although the equivalent conductivity approximation is still not so good.

As intraparticle diffusion becomes dominant (the Biot number increases) the finite stage and continuous models become similar to each other while when the curve spread parameter is small (and hence also the skewness of the curves) the sensitivity of the plots to Biot number decreases.

SIMPLIFIED METHOD OF BREAKTHROUGH CURVE PREDICTION

In Figure 1 the standard deviation given by Equation (15) has been used as the single parameter correlating points on breakthrough curves for various parameter combinations.

The computations of Figure 1 were carried out by a further development of a Hermite polynomial method of Fourier transform inversion previously presented in (*13*).

The further developments (which make the method a more practical one) involve automatic selection of the scale factor Z for the approximation and use of the general integral formula for breakthrough curve prediction presented in (*12*). Details of the procedure are given in Appendix 2.* Tables of the coefficients a_n in the Hermite polynomial expansions are given in (*14*). Since the curves are relatively insensitive to V_H for V_H large, all the computations have been carried out at a fixed value of V_H of 1,000.

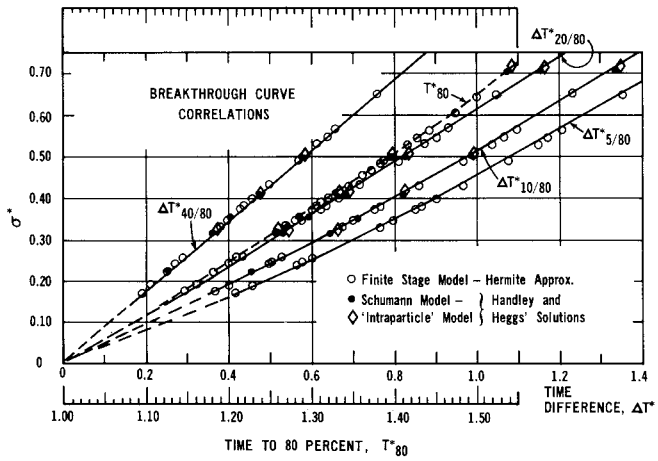

Fig. 1. Correlation of normalized time differences for breakthrough curves: Normalized time differences ΔT^* against normalized standard deviation σ^* and normalized time to 80 p.c. against σ^*.

* See footnote on page 413.

TABLE 5. COEFFICIENTS b_n IN POLYNOMIALS OF EQUATION (22)
$V_H = 1000$

Schumann, Rosen and Finite Stage Models

Normalized time	b_0	b_1	b_2	b_3	Error std. dev. in predicted values
T^*_{05}	0.9985	−1.7105	0.0254	0.0532	0.00210
T^*_{10}	0.9980	−1.3020	0.2776	−0.0340	0.00192
T^*_{20}	0.9980	−0.8551	0.0132	−0.0430	0.00144
T^*_{40}	0.9999	−0.2504	−0.2488	0.0221	0.00071
T^*_{80}	1.0046	0.7874	0.0430	−0.1222	0.01300

TABLE 6. COEFFICIENTS c_n IN POLYNOMIALS OF EQUATION (23)
$V_H = 1000$

Schumann, Rosen and Finite Stage Models

Normalized time diff.	c_0	c_1	c_2	c_3	Error standard dev. in predicted values
$\Delta T^*_{05/80}$	0.0030	0.3890	0.0005	0.0234	0.0090
$\Delta T^*_{10/80}$	−0.0029	0.4862	0.0031	0.0232	0.0068
$\Delta T^*_{20/80}$	−0.0034	0.6162	−0.0309	0.0263	0.0080
$\Delta T^*_{40/80}$	0.0024	0.9677	−0.2672	0.1548	0.0111

The fitting of third degree polynomials through the breakthrough point allows the times T^*_{05}, T^*_{10}, T^*_{20}, T^*_{40} and T^*_{80} to be estimated where the subscripts refer to the 5%, 10%, 20%, etc. of completed response points on the curves. The general form is

$$T^* = b_0 + b_1\sigma^* + b_2\sigma^{*2} + b_3\sigma^{*3} \qquad (22)$$

Further correlations of other times could be developed using the tabulated coefficients a_n referred to above.

Since for $\sigma^* = 0$, all times T^* should be unity, the coefficients b_0 should all be unity. Slight deviations do occur as shown in Table 5. In obtaining the least squares polynomial fits of Equation (22) the Schumann and Rosen model computations of Handley and Heggs were included and all Hermite polynomial approximations having an integral error-square greater than 2×10^{-6} were excluded. A knowledge of the integral error square is a useful feature of the Hermite polynomial approximation procedure.

SIMPLIFIED METHOD OF EXPERIMENTAL DATA ANALYSIS

The alternative problem of rapidly determining values of σ^* from an experimental breakthrough curve may also be simplified in a similar manner. Thus, least squares polynomials may be fitted to the time differences on either side of the stoichiometric breakthrough time. In this paper, the correlations are between the 80% point on a curve and the 5, 10, 20, and 40% points (denoted $\Delta T^*_{10/80}$ etc.) although other empirical correlations such as $\Delta T^*_{05/95}$, $\Delta T^*_{10/90}$, etc. could also be developed.

In its application to experimental work, the center of mass or stoichiometric breakthrough time $\mu(t)$ is calculated. Times are then normalized with respect to $\mu(t)$ and

a number of estimates made of σ^* from Equation (23) with coefficients given in Table 6.

$$\sigma^* = c_0 + c_1 \cdot \Delta T^* + c_2 (\Delta T^*)^2 + c_3 (\Delta T^*)^3 \quad (23)$$

It may also be noted that since for zero curve spread parameter σ^* time differences ΔT^* should be zero, the coefficients c_0 in Table 6 should also be zero.

CONCLUSIONS AND FURTHER WORK

The analysis of this paper shows that internal particle conduction is predicted to have two effects, one on breakthrough curve dispersion or spread and the other on curve shape. The relative importance of internal particle conduction is predicted in each case to depend only on the Biot number Bi (assuming a constant heat transfer parameter Y).

The importance of heat capacity ratio V_H has been theoretically demonstrated. It appears that for high values of V_H the Schumann model should provide a good description of packed bed dynamics, provided axial dispersion and intraparticle effects are lumped into an equivalent or pseudo heat transfer parameter Y_p given by

$$\frac{1}{Y_p} = \frac{1}{NPe} + \frac{1 + Bi/5}{Y} \cdot \beta^2 \quad (24)$$

The equivalent conductivity model appears to be valid only for very low values of heat capacity ratio corresponding to a poorly "adsorptive" packing. Integral square of the deviation computations suggest that the model is not a particularly good approximation to the more complex models even at low V_H values.

Use of empirical correlations of curve spread parameter against time differences in a breakthrough curve allow these curves to be rapidly estimated and have been used in the experimental work reported in the companion paper to this (*23*).

Extension of the methods of analysis in this paper to the more complex situations involving finite adsorption rate in mass transfer work (*20*) and fluid-solid-fluid axial conduction in heat transfer (*16*) should be of value.

NOTATION

a_p = surface to volume ratio of a particle, ft.$^{-1}$
Bi = fluid particle Biot number = Rh_p/k_s for heat transfer
b_n = nth coefficient in empirical breakthrough curve correlation, Equation (22)
c_f, c_s = heat capacity of fluid and solid, respectively, B.t.u./(lb.)(°F.)
c_n = nth coefficient in empirical breakthrough curve correlation, Equation (23)
D_e = fluid phase axial dispersion coefficient, sq.ft./hr.
d_p = particle diameter
$g(t)$ = impulse response, here response of exit fluid to impulsive change in inlet fluid temperature
$G(j\omega)$ = frequency response transfer function or Fourier transform of impulse response
h_p = surface-averaged fluid particle heat transfer coefficient, B.t.u./(hr.)(sq.ft.)(°F.)
k_f, k_s = thermal conductivity of fluid and solid phases respectively, B.t.u./(hr.)(ft.)(°F.)
L = bed length, ft.
M_f, M_s = total mass of fluid and solid respectively in packed bed, lb.
M = equivalent number of mixing stages, finite stage model
N = bed length in particle diameters = L/d_p
Pe, Pe' = equivalent fluid phase axial dispersion Peclet numbers with particle diameter and bed length as characteristic lengths, respectively
Pe_a = overall equivalent conductivity model Peclet number
r = normalized radial distance in a particle, $0 < r < 1$
R = particle radius, ft.
Re_p = superficial particle Reynolds number, d_pG/μ_f
St = fluid-particle Stanton number, h_p/Gc_f
t, t^* = time, normalized relative to mean fluid holdup time L/v_a and relative to first moment of impulse response $\mu(t)$, respectively
$\Delta T^*_{05/80}$ = time taken between 5% and 80% of completed response on a breakthrough curve, normalized relative to first absolute moment of impulse response density function $g(t)$
T_p = or $T_p(z, r, t)$ temperature within a particle
T = or $T(z, t)$ fluid temperature distance z, time t
T_i = or $T_i(t)$ inlet fluid temperature uniform across section
v_a = mean interstitial fluid velocity ft./hr.
V_H = heat capacity ratio, Equation (4)
W = total weight flowrate of fluid through bed, lb./hr.
x = used only as part of compound symbol, $\gamma x = Y/Bi$
Y = heat transfer parameter, $6NSt(1 - \epsilon)$ for spherical or right cylindrical particles
Y_p = "pseudo" value of heat transfer parameter, incorporating effects of internal particle heat transfer resistance
Y_{calc} = apparent heat transfer parameter incorporating effects of axial fluids dispersion
z = distance from bed inlet normalized relative to bed length L

Greek Letters

γ = used with x as compound symbol $\gamma x = Y/Bi$ bed length parameter of Babcock and of Rosen
γ_1 = statistical measure of skewness of impulse response (density) function $g(t)$, $\gamma_1 = \pi^{*3}/\sigma^{*3}$
ϵ = mean volumetric porosity of bed
$\epsilon(t)$ = deviation between impulse responses of two models
κ_n = nth cumulant of impulse response density function and *defined* by

$$\ln G(j\omega) = \sum_{n=0}^{\infty} \kappa_n \frac{(-j\omega)^n}{n!}$$

κ_n^* = nth cumulant normalized with respect to first absolute moment $\mu_1'(t)$ of impulse response density function
μ_n' = nth absolute moment of impulse response normalized with respect to mean fluid holdup time, L/v_a
$\mu(t)$ = first absolute moment or center of mass of $g(t)$ in time units, hr.
π^{*3} = third central moment of impulse response density function = κ_3^*, normalized relative to $\mu(t)$
ρ_s, ρ_f = density of fluid and solid packing respectively, lb./cu.ft.
σ^* = curve spread parameter, standard deviation of impulse response density function $g(t)$ normalized relative to center of mass, $\mu(t)$ where $\sigma^{*2} = \kappa_2^*$
ω^* = natural frequency normalized relative to $\mu(t)$
γx = "bed length parameter" = $Y/Bi = Y_{calc}/Bi_{calc}$
β = ratio, $V_H/(V_H + 1)$

LITERATURE CITED

1. Antonson, C. R., and P. S. Dranoff, *Chem. Eng. Progr. Symposium Ser., 63*, **74**, 61 (1967).
2. Babcock, R. E., D. W. Green, and R. H. Perry, *AIChE J.*, **12**, 922 (1966).
3. Babcock, R. E., R. H. Perry, and O. K. Crosser, *Chem. Eng. Progr. Symp. Ser., 63*, **77**, 102 (1967).
4. Bradshaw, A. V., A. Johnson, N. H. McLachlan, and Y-T. Chiu, *Trans. Inst. Chem. Engrs. (London)*, **48**, T77 (1970).
5. Chao, R., and H. E. Hoelscher, *AIChE J.*, **12**, 271 (1966).
6. Denton, W. H., *Proc. of General Disc. on Heat Transfer*, Inst. Mech. Engrs. (London) and ASME, 370 (1951).
7. Edwards, J. F., and J. F. Richardson, *Chem. Eng. Sci.*, **23**, 109 (1968).
8. Handley, D., and P. J. Heggs, *Trans. Inst. Chem. Engrs. (London)*, **46**, T251.
9. *Ibid., Inst. J. Heat Mass Trans.*, **12**, 549 (1969).
10. Hays, J. R., W. C. Clements, Jr., and T. R. Harris, *AIChE J.*, **13**, 374 (1967).
11. Jeffreson, C. P., *Chem. Eng. Sci.*, **24**, 613 (1969).
12. *Ibid.*, **25**, 1319 (1970).
13. Jeffreson, C. P., *Inst. Engrs. of Australia Elec. Eng. Trans.*, **EE5**, 77 (1969).
14. *Ibid.*, Ph.D. thesis, University of Adelaide, Australia (1971).
15. Kucera, E., *J. Chromatog.*, **19**, 237 (1965).
16. Littman, H., R. G. Barille, and A. H. Pulsifer, *Ind. Eng. Chem. Fundamentals*, **7**, 554 (1968).
17. Rosen, J. B., *J. Chem. Phys.*, **20**, 287 (1952).
18. Sagara, M., P. Schneider, and J. M. Smith, *Chem. Eng. J.*, **1**, 47 (1970).
19. Schumann, T. E. W., *J. Franklin Inst.*, **208**, 405 (1929).
20. Schneider, P., and J. M. Smith, *AIChE J.*, **14**, 762 (1968).
21. McAdams, W. H., "Heat Transmission," Third Ed., McGraw-Hill, New York (1954).
22. Hotta, K., *Kagaku Kogaku* (Abr. Eng. Edn), **3**, 4 (1965).
23. Jeffreson, C. P., *AIChE J.*, **18**, (1972).

II. Experimental Evidence for Axial Dispersion and Intraparticle Effects

The effects of axial fluids dispersion on breakthrough curves in packed beds is considered and formulae are derived for 'F-factors', which allow heat transfer coefficients obtained by step testing to be corrected for axial fluids dispersion. A comparison of steady state and unsteady correlations for heat transfer in packed beds suggests that axial dispersion effects are incorporated in certain steady state heat transfer correlations. Further correction would thus lead to errors in breakthrough curve prediction. Experimental data for breakthrough curves in packed beds of highly conductive and poorly conductive spheres is examined and Biot number correction factor $1 + Bi/5$ shown to be valid for Biot numbers up to about 4.

Part I of this paper (*8*) presents simplified theoretical methods of predicting breakthrough curves in linear adsorbers and thermal regenerators, allowing for axial fluids dispersion. Unfortunately, experimental evidence for the effects of axial fluids dispersion on packed bed dynamics is inconclusive and difficult to interpret. Reasons for this are examined in this paper.

Particle internal conduction effects are more easily predicted and measured. Experimental evidence for the validity of the $1 + Bi/5$ correction factor suggested by Bradshaw et al. (*12*) and discussed in Part I of the paper is examined using the extensive results of Handley and Heggs (*7*) together with some confirmatory results of the writer.

AXIAL DISPERSION EFFECTS–EXPERIMENTAL DIFFICULTIES

The integral deviation square computations of Part I (*8*) suggest that experimentally the effects of axial fluids dispersion may be difficult to separate from that due to fluid-particle heat transfer resistance in the analysis of breakthrough curves in packed beds. This is because the predicted deviations between various models of packed bed dynamics due to axial fluids dispersion are generally less than would arise from experimental errors. As an example, Table 1 shows the integral deviation square between impulse responses predicted by the Schumann model, (which ignores axial fluid dispersion) and the continuous, axial dispersion model with simplified boundary conditions of Chao and Hoelscher (*13*) discussed in Part I of this paper. The comparison is at a fixed normalized variance σ^{*2} of 0.125, a heat capacity ratio V_H of 10^4 and a Biot number of zero.

An integral deviation square of 5.4×10^{-4} (obtained when axial dispersion contributes 40% to total variance σ^{*2}) would be extremely difficult to distinguish from experimental 'noise' and other inaccuracies.

Nonetheless, the effects of axial dispersion could be distinguished from fluid-solid heat transfer if an accurate heat transfer coefficient correlation (obtained by methods which are free from axial dispersion) were available. Any increase in breakthrough curve dispersion over that pre-